J. Fluid Mech. (1975), *vol.* 74, *part* 4, *pp.* 685–694
Printed in Great Britain

Single-wave run-up on sloping beaches

By LESTER Q. SPIELVOGEL
Joint Tsunami Research Effort, Pacific Marine Environmental Laboratory,
N.O.A.A., Honolulu, Hawaii 96822

(Received 29 October 1974)

Possibilities of high shoreline amplification and run-up are investigated. A shoreline amplification of magnitude 5·38 and a tsunamigenic (deep water) amplification of magnitude 5·71 are obtained from single waves without analytic or computational difficulties. It is not claimed that these are a maximum, but rather it is conjectured that arbitrarily high run-up and amplification can be obtained provided that the correct initial wave trains are chosen.

In studies of wave damage due to tsunamis and storm waves, it is of interest to predict the run-up of these waves on the shoreline of a sloping beach. Also, the existence of a maximum amplification over a class of incoming wave trains has been questioned and still is unresolved.

Carrier & Greenspan (1958) performed such an analysis using a shallow-water theory. They assumed specific initial wave shapes with initial velocity zero and then analysed the wave shape and run-up as the waves propagated towards the shore.

In Carrier & Greenspan (1958) and later in Butler (1967), initial waves divide into seagoing and run-up waves. The run-up is then the result of two wave packets rather than a single wave packet. This causes some ambiguity in wave-train identification which can be corrected with some difficulty by assigning the proper non-zero velocity to the initial packet so that it all propagates towards the shoreline. A simpler alternative scheme is used in this paper.

We shall consider an inverse problem and calculate the wave shape using run-up data as the initial state. In this case an initial velocity equal to zero is interpreted to mean that all the kinetic energy of the wave has been transformed into the potential energy of the run-up. By taking run-up data as initial data, we clear up the ambiguity in wave-train identification. There is still some ambiguity in defining amplification since the wave shape causing run-up is not known initially. We are able, however, to define it in a logical way once we allow the wave shapes to evolve through the magic of the differential equations.

Let us consider two-dimensional flow over an inclined beach (see figure 1). If V^*, η^*, x^* and t^* are the dimensional velocity, surface elevation, abscissa and time, let unstarred symbols represent the dimensionless quantities according to

$$V^* = V_0 V \equiv (gL\beta)^{\frac{1}{2}} V, \quad \eta^* = \beta L \eta, \quad x^* = Lx \tag{1}$$

and

$$t^* = Tt \equiv (L/\beta g)^{\frac{1}{2}} V,$$

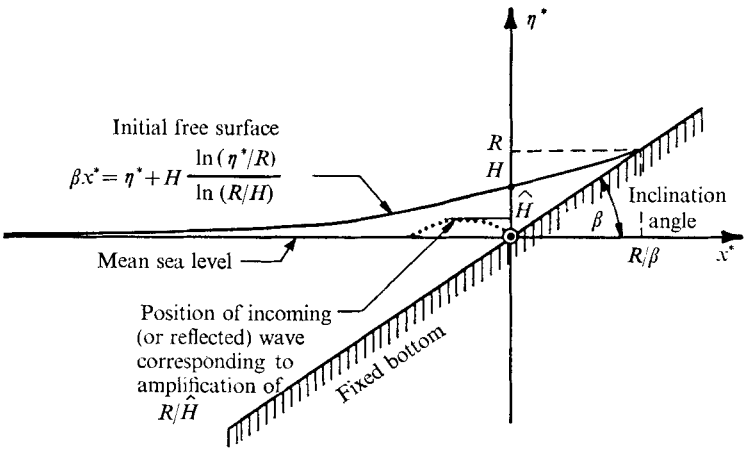

FIGURE 1. Physical geometry and co-ordinate system showing initial wave and wave at shoreline.

where L is a typical length, β is the beach slope and g is the acceleration due to gravity. We shall solve the shallow-water problem given by

$$\left.\begin{aligned} \frac{\partial[V^*(\eta^*+h^*)]}{\partial x^*} &= -\frac{\partial \eta^*}{\partial t^*}, \\ \frac{\partial V^*}{\partial t^*} + V^*\frac{\partial V^*}{\partial x^*} &= -g\frac{\partial \eta^*}{\partial x^*}, \end{aligned}\right\} \tag{2}$$

where, in this case, $h^*(x^*)$ is the water depth βx^*. The differential equations for the dimensionless problem are the same as (2) with the stars suppressed and g set equal to unity. We shall transform the problem from the x, t plane to the σ, λ plane using

$$V = \sigma^{-1}\partial\phi(\sigma,\lambda)/\partial\sigma, \quad x = \tfrac{1}{4}\partial\phi/\partial\lambda - \tfrac{1}{2}V^2 - \tfrac{1}{16}\sigma^2, \tag{3), (4}$$

$$\eta = \tfrac{1}{4}\partial\Phi/\partial\lambda - \tfrac{1}{2}V^2, \quad t = \tfrac{1}{2}\lambda - V, \tag{5), (6}$$

where $\sigma \geqslant 0$. The instantaneous shoreline is $\sigma = 0$ while $\lambda = 0$ represents the initial time for the problem posed here. The differential equations of this shallow-water theory transform into

$$\left(\frac{\partial^2}{\partial\lambda^2} - \frac{\partial^2}{\partial\sigma^2} - \frac{3}{\sigma}\frac{\partial}{\partial\sigma}\right)V = 0, \tag{7}$$

or

$$\left[\frac{1}{\sigma}\frac{\partial}{\partial\sigma}\left(\sigma\frac{\partial}{\partial\sigma}\right) - \frac{\partial^2}{\partial\lambda^2}\right]\phi = 0. \tag{8}$$

In order to transform back into x, y co-ordinates, we must specify that the Jacobian

$$\partial(x,t)/\partial(\sigma,\lambda) = \tfrac{1}{4}\sigma[V_\sigma^2 - (\tfrac{1}{2} - V_\lambda)^2] \tag{9}$$

is non-zero in the appropriate domain. The solution of (8) derived in Carrier & Greenspan (1958) is given by

$$\phi = -\int_0^\infty \frac{1}{\tau}J_0(\tau\sigma)\sin(\tau\lambda)\,I(\tau)\,d\tau, \tag{10}$$

where

$$I(\tau) = \int_0^\infty 4\sigma J_1(\sigma\tau)\,(\eta_0)_\sigma\, d\sigma, \tag{11}$$

and

$$\eta_0(\sigma) = \eta(\sigma, 0) \tag{12}$$

is the initial shape. Rather than (10), we shall be interested in the derived formulae

$$\eta_1(\sigma, \lambda) = \frac{\phi_\lambda}{4} = -\frac{1}{4}\int_0^\infty J_0(\tau\sigma)\cos(\tau\lambda)\, I(\tau)\, d\tau \tag{13}$$

and

$$V(\sigma, \lambda) = \int_0^\infty \frac{1}{\sigma} J_1(\tau\sigma)\sin(\tau\lambda)\, I(\tau)\, d\tau. \tag{14}$$

We shall consider the initial run-up shape implicitly defined by

$$\ln\frac{\eta^*(x^*, 0)}{R} = \ln\left(\frac{R}{H}\right)\frac{\beta x^* - \eta^*}{H}. \tag{15}$$

As one can see in figure 2, R is the run-up amplitude and H the height of this wave at the steady-state shoreline ($x^* = 0$). In the unstarred co-ordinate system (15) is reduced to

$$\eta(x, 0) = A\exp[16p(x - \eta_0)], \tag{16}$$

or

$$\eta_0 = \eta(\sigma, 0) = A\exp(-p\sigma^2), \tag{17}$$

where

$$R = A\beta L > 0 \tag{18}$$

and

$$16Ap = \frac{R}{H}\ln\frac{R}{H} > 0 \tag{19}$$

define the constants A and p in terms of R and H.

Essentially this is an exponentially shaped run-up. Values of A and p must be limited to those yielding a non-zero Jacobian (9). With this initial state we proceed to evaluate the kernel (11) and get

$$I(\tau) = -(2A/p)\exp(-\tau^2/4p). \tag{20}$$

The solution integrals then become

$$V = -\frac{2A}{\sigma p}\int_0^\infty \tau\exp(-\tau^2/4p)\, J_1(\tau\sigma)\sin(\tau\lambda)\, d\tau, \tag{21}$$

$$\eta_1 = -\frac{\phi_\lambda}{4} = \frac{A}{2p}\int_0^\infty \tau\exp(-\tau^2/4p)\, J_0(\tau\sigma)\cos(\tau\lambda)\, d\tau, \tag{22}$$

$$\eta = \eta_1 - \tfrac{1}{2}V^2, \quad t = \tfrac{1}{2}\lambda - V. \tag{23), (24}$$

The above solutions may be written in several other forms for numerical analysis.

The series

$$\eta_1 = A\sum_{k=0}^{\infty}\sum_{s=0}^{\infty}\frac{(-4p\lambda^2)^s(-p\sigma^2)^k(s+k)!}{2s!\,k!\,k!} \tag{25}$$

and
$$V = -8pA\lambda \sum_{k=0}^{\infty} \sum_{s=0}^{\infty} \frac{(-4p\lambda^2)^s (-p\sigma^2)^k (s+k+1)!}{(2s+1)!\,(k)!\,(k+1)!} \tag{26}$$

are everywhere convergent but because of round-off errors they are useful numerically only when $p\sigma^2$ and $p\lambda^2$ are small. This is the form we found to be best for determining near-shore amplification. Both series may be computed simultaneously upon noting the ratio of corresponding terms.

Another useful representation of the solution may be evaluated after tabulating the function

$$f(\alpha) = \alpha^2 \int_0^{\alpha} \exp[-\alpha^2(1-y^2)]\,dy = \frac{\alpha\pi^{\frac{1}{2}}}{2} \operatorname{erf}(-i\alpha)$$

$$= \alpha^2 \sum_{n=0}^{\infty} \frac{(-4^{\alpha^2})^n n!}{(2n+1)!} = \exp(-\alpha^2) \sum_{n=0}^{\infty} \frac{\alpha^{2n+2}}{(2n+1)\,n!}. \tag{27}$$

For completeness we note that

$$\lim_{\alpha \to \infty} f(\alpha) = \tfrac{1}{2}. \tag{28}$$

In terms of $f(\alpha)$ we have

$$\eta_1 = \frac{A}{\pi} \int_0^{\pi} [1 - f(\alpha_+) - f(\alpha_-)]\,d\phi \tag{29}$$

and
$$V = \frac{4A}{\pi\sigma} \int_0^{\pi} \sin\phi [f(\alpha_-) - f(\alpha_+)]\,d\phi, \tag{30}$$

where
$$\alpha_{\pm}^2 = p(\sigma \sin\phi \pm \lambda)^2. \tag{31), (32}$$

From these formulae we see that, as time progresses, η_1, V and η will become essentially zero except in neighbourhoods where $\sigma/\lambda \sim 1$ and as expected we get a single wave train in the neighbourhood of $x \sim -\frac{1}{4}t^2$ or $x^* \sim -\frac{1}{4}\beta g t^{*2}$. This form of the solution is useful in tracking the waves into the deeper ocean.

We can also evaluate the shoreline behaviour directly from (27). We have

$$\eta_1(\lambda, 0) = A[1 - 2f(\lambda p^{\frac{1}{2}})] \tag{33}$$

and
$$V(\lambda, 0) = -4A\lambda p[1 + (1/\lambda^2 p - 2) f(\lambda p^{\frac{1}{2}})], \tag{34}$$

which can likewise be computed in terms of tabulated error functions of imaginary argument:

$$\eta_1(\lambda, 0) = A[1 - i\pi^{\frac{1}{2}} \lambda p^{\frac{1}{2}} \operatorname{erf}(-i\lambda p^{\frac{1}{2}})] \tag{35}$$

and
$$V(\lambda, 0) = -4Ap\left[\lambda + \frac{(1 - 2\lambda^2 p)\, i\pi^{\frac{1}{2}}}{2p^{\frac{1}{2}}} \operatorname{erf}(-i\lambda p^{\frac{1}{2}}).\right] \tag{36}$$

We have done some numerical calculations based on (25) and (26). The important dimensional constants are R, the height of the maximum run-up, and H, the height of the run-up wave at the origin (see figure 2). Equations (18) and (19) relate these to the constants A and p used in the computational scheme. Let us also note that R/H becomes the important dimensionless parameter that identifies the wave shape.

For consideration of computational accuracy we also need to know that

$$p\lambda^2 = \frac{\beta^2 g}{4H} \ln\left(\frac{R}{H}\right)\left(t^* + \frac{V^*}{\beta g}\right)^2, \tag{37}$$

and

$$p\sigma^2 = \frac{\eta^* - \beta x^*}{H} \ln\frac{R}{H} \equiv \frac{H^*}{H} \ln\frac{R}{H}, \tag{38}$$

which appear in the power-series solution given by (25) and (26).

It is obvious that large times t^* or large total depths H^* make the corresponding left-hand sides of (37) and (38) large, implying less computational accuracy because of round-off errors. One also sees the advantage of considering R/H to be close to unity. This corresponds to very long initial waves, for instance, tsunamigenic waves; this also corresponds to the region of validity of this shallow-water theory. By taking $R/H \sim 1$, we reduce the values of $p\lambda^2$ and $p\sigma^2$ and thus may extend our computations to longer times and larger distances. In all the calculations performed, there was no problem in seeing the wave begin to form and depart from the shoreline. In all cases, we found that the exponential run-up was caused by a leading negative wave followed by a positive wave. That this is true at the shoreline is evident from (33) and (34).

Since we have well-defined wave forms, we are able to define amplification. Consider the approaching (or receding) wave at the position where the height at the shoreline is zero. The ratio of the run-up amplitude R to the maximum height $\hat{H}$ of the wave in this position will be the amplification (or shoreline amplification). This is well defined for the initial conditions here and corresponds closely to the previously mentioned papers on the subject (see dotted curve in figure 1).

While the previously cited references found shoreline amplifications of 1·45 (Carrier & Greenspan 1958) and 2·33 (Butler 1967), we have had no difficulty in attaining 5·38. Figures 2–7 show some sample wave forms. The initial curves (for $t^* = 0$) show exponential run-up. Since the sequence is symmetric about zero time, the approaching wave is the same shape as the run-down wave but at a negative time. As R/H increases we get both multiple-valued solutions and physically unrealistic solutions.

A curve of shoreline amplification *vs.* R/H is given in figure 8; the corresponding data are in table 1. The three regions in figure 8 correspond to different behaviour of the Jacobian. The left-hand region exhibits a reasonably shaped, single-valued solution from $t = -\infty$ to $t = +\infty$ for all x. The middle region corresponds to Jacobian breakdown (multiple-valued solutions) as the wave progresses away from the shoreline, i.e. for some $x < 0$ but for no $x > 0$. The right-hand region (waves of shorter wavelength) corresponds to Jacobian breakdown while the wave is forming, running down the slope. Only the left and middle sections contain useful information regarding water waves. The right-hand section is there for mathematical interest.

We do not wish to imply that the high amplitudes we have obtained are maximum or near maximum. One can get higher values if one wishes by taking initial shapes which differ from the one used here [equations (15)–(17)].

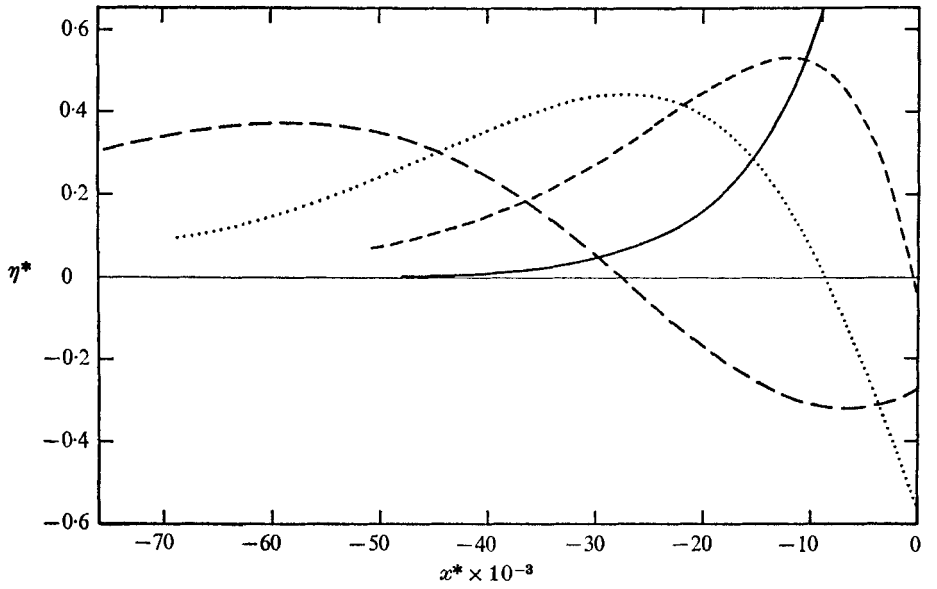

FIGURE 2. Case 1. $R = 2{\cdot}0$, $H = 1{\cdot}99$, amplification = 3·74. ——, $t^* = 0$; – – –, $t^* = 243$; · · · · ·, $t^* = 386$; — —, $t^* = 600$.

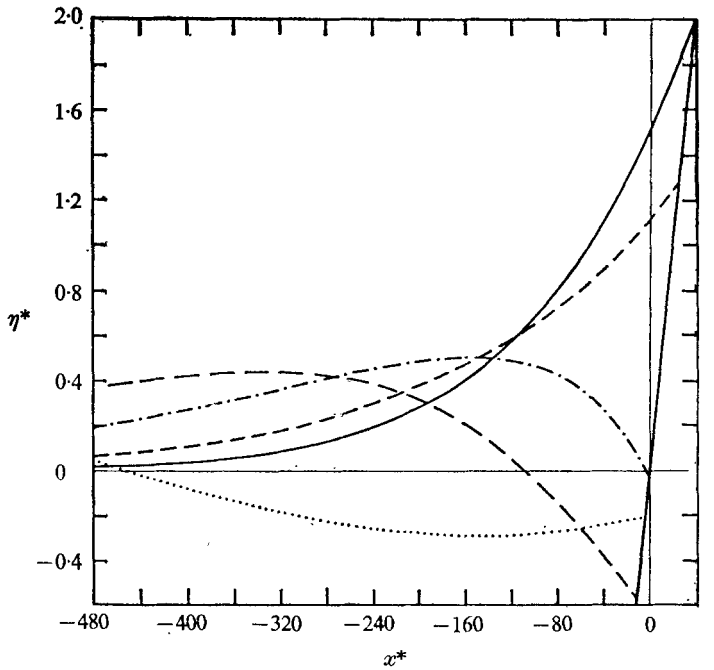

FIGURE 3. Case 2. $R = 2{\cdot}0$, $H = 1{\cdot}5$, amplification = 3·98. ——, $t^* = 0$; – – –, $t^* = 15$; —·—, $t^* = 29$; — —, $t^* = 44$; · · · · ·, $t^* = 75$.

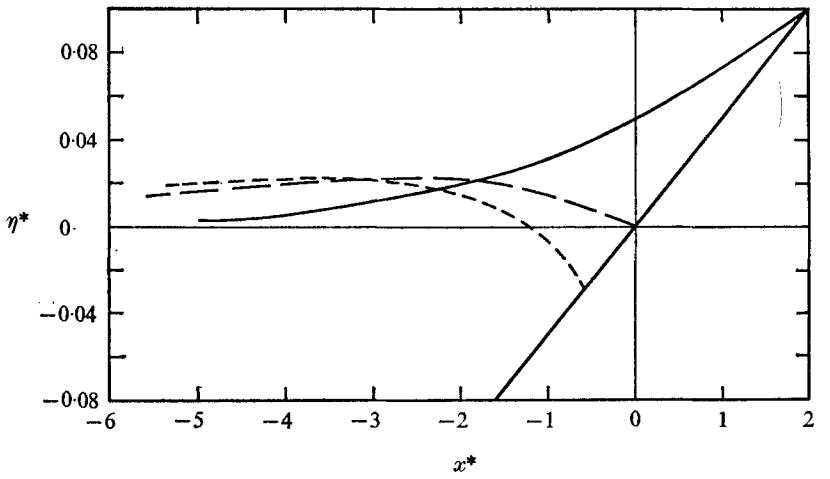

FIGURE 4. Case 4. $R = 0{\cdot}1$, $H = 0{\cdot}05$, amplification = 4·56. ——, $t^* = 0$; — —, $t^* = 0{\cdot}4$; – – –, $t^* = 0{\cdot}5$.

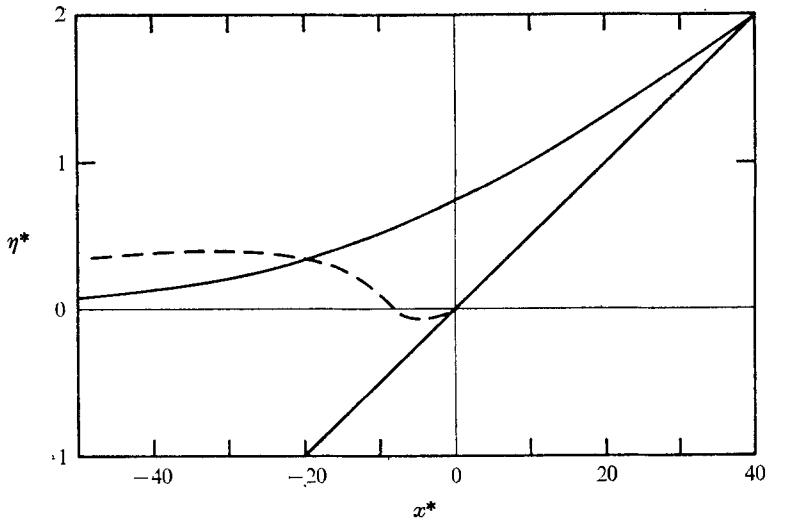

FIGURE 5. Case 5. $R = 2{\cdot}0$, $H = 0{\cdot}75$, amplification = 5·15. ——, $t^* = 0$; — —, $t^* = 15{\cdot}3$.

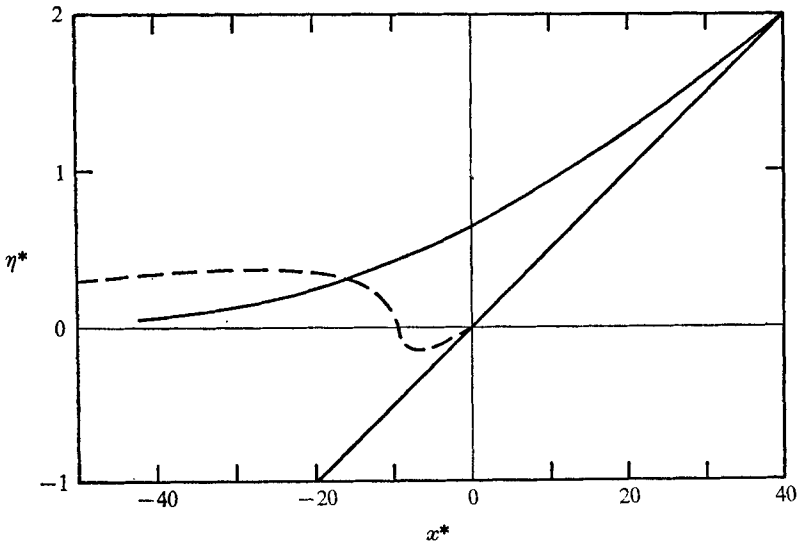

FIGURE 6. Case 6. $R = 2{\cdot}0$, $H = 0{\cdot}655$, amplification = 5·381. ——, $t^* = 0$; — —, $t^* = 14{\cdot}7$.

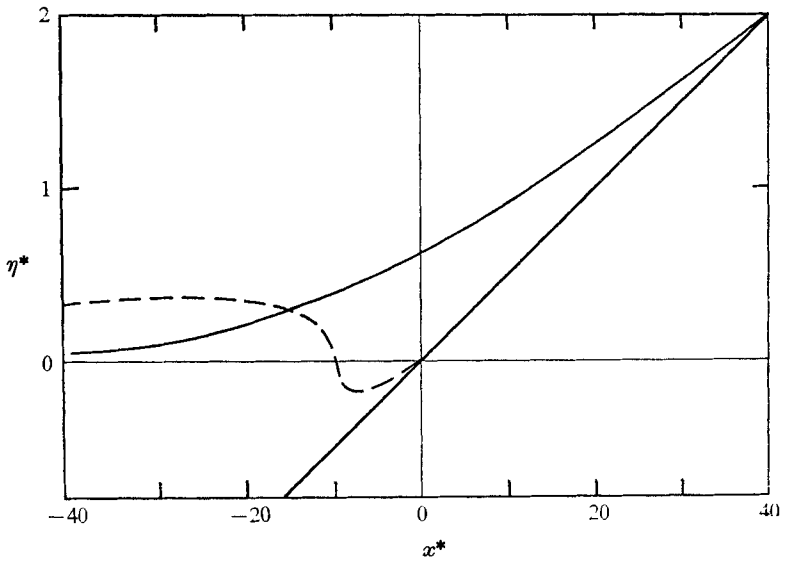

FIGURE 7. Case 7. $R = 2{\cdot}0$, $H = 0{\cdot}625$, amplification = 5·51. ——, $t^* = 0$; — —, $t^* = \pm 14{\cdot}5$.

Case	1	2	3	4	5	6	7	8
Figure	2	3	—	4	5	6	7	—
R	2	2	2	0·1	2	2	2	2
H	1·99	1·5	1	0·05	0·75	0·655	0·625	0·5
β	$\frac{1}{20}$	$\frac{1}{20}$	$\frac{1}{20}$	$\frac{1}{20}$	$\frac{1}{20}$	$\frac{1}{20}$	$\frac{1}{20}$	$\frac{1}{20}$
p	$7{\cdot}872 \times 10^{-6}$	$5{\cdot}993 \times 10^{-4}$	$2{\cdot}166 \times 10^{-3}$	0·0433	$4{\cdot}087 \times 10^{-3}$	$5{\cdot}326 \times 10^{-3}$	$5{\cdot}816 \times 10^{-3}$	$8{\cdot}664 \times 10^{-3}$
T_0	1·4286	1·4286	1·4286	1·4286	1·4286	1.4286	1·4286	1·4286
V_0	0·7000	0·7000	0·7000	0·7000	0·7000	0·7000	0·7000	0·7000
R/H	1·0050	1·3333	2·0000	2·0000	2·6667	3·0534	3·2000	4·0000
Amplification	3·74	3·98	4·56	4·56	5·15	5·3814	5·51	5·58
Amplification at 3 km depth	5·71	—	—	—	—	—	—	—

TABLE 1. Data for examples illustrated

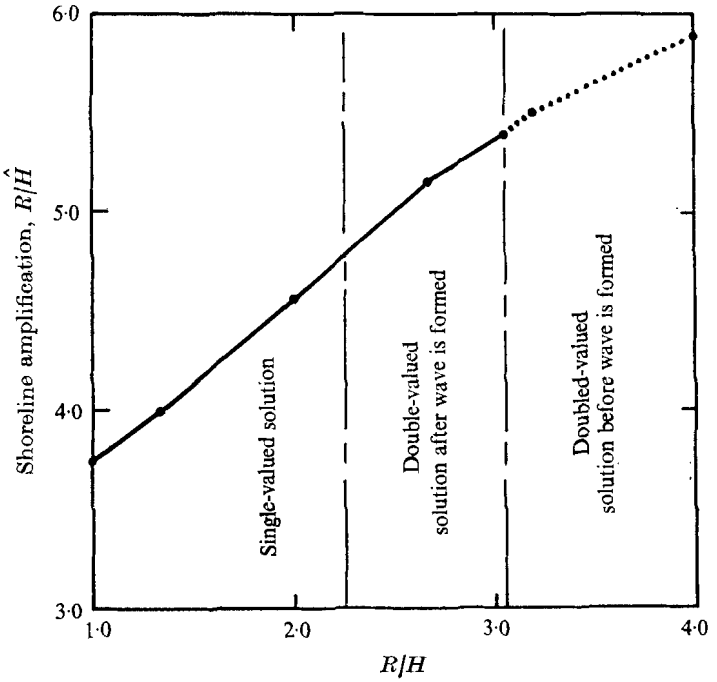

FIGURE 8. Shoreline amplification $R/\hat{H}$ as function of R/H.

With regard to tsunamis the amplifications calculated here are only one factor. Basically we have computed some near-shore amplifications. These must be modified (increased) by the amplification involved while the wave evolves from oceanic to near-shore depths. This again must be modified (increased) by the amplification due to near-shore focusing (three-dimensional effects). For tsunamis the total product of these amplifications may reach a possible maximum in the range 25–40.

REFERENCES

BUTLER, J. P. 1967 *Hawaii Inst. Geophys., University of Hawaii, Rep.* HIG-67-16.

CARRIER, G. F. & GREENSPAN, H. P. 1958 *J. Fluid Mech.* **4**, 97.